

# Ginsenoside Rg2 protects cardiomyocytes against trastuzumab-induced toxicity by inducing autophagy

GUANG LIU<sup>1</sup>, XIAOYONG QI<sup>2</sup>, XINGTAO LI<sup>3</sup> and FANGYI SUN<sup>3</sup>

<sup>1</sup>Department of Cardiovascular Medicine, Hebei Medical University; <sup>2</sup>Department of Cardiovascular Medicine, Hebei General Hospital; <sup>3</sup>Department of Cardiovascular Medicine, The Fourth Affiliated Hospital of Hebei Medical University, Shijiazhuang, Hebei 050000, P.R. China

Received August 9, 2019; Accepted February 25, 2020

DOI: 10.3892/etm.2021.9904

**Abstract.** Trastuzumab (TzM) significantly improves the outcomes of patients with breast cancer; however, it is associated with severe cardiotoxicity. Ginsenoside Rg2 was reported to exert protective effects against myocardial injury and apoptosis in human cardiomyocytes (HCMs). However, whether ginsenoside Rg2 protects HCMs against TzM-induced toxicity remains unclear. The present study investigated the proliferation of HCMs using a Cell Counting Kit-8 assay and Ki67 immunofluorescence staining. Apoptotic cells were detected by Annexin V/propidium iodide staining and flow cytometry. Furthermore, monodansylcadaverine staining was performed to detect cell autophagy. In addition, western blotting was used to detect the expression levels of phosphorylated (p)-Akt, p-mTOR, beclin 1, microtubule associated protein 1 light chain 3 $\alpha$  (LC3) and autophagy protein 5 (ATG5) in HCMs. Pretreatment with ginsenoside Rg2 significantly protected HCMs against TzM-induced cytotoxicity by inhibiting apoptosis. Furthermore, pretreatment with ginsenoside Rg2 induced autophagy in HCMs by upregulating the expression levels of p-Akt, p-mTOR, beclin 1, LC3 and ATG5. The results obtained in the present study suggested that ginsenoside Rg2 could protect HCMs against TzM-induced cardiotoxicity by activating autophagy. Therefore, ginsenoside Rg2 may serve as a potential therapeutic agent to prevent TzM-related cardiotoxicity in patients with breast cancer.

## Introduction

Ginseng (*Panax ginseng*) is a traditional Chinese herbal medicine that has been widely used for thousands of years in East Asia, including China, Korea and Bhutan (1). The main components responsible for its therapeutic effects are ginsenosides, which

are divided into protopanaxadiol and protopanaxatriol ginsenoside groups (2). Ginsenoside Rg2 is one of the compounds in the protopanaxatriol group (3). Ginsenoside Rg2 improved neurological performance and enhanced memory by inhibiting neuronal apoptosis in a rat model of vascular dementia (3). Ginsenoside Rg2 improved neuronal and metabolic activities by inducing autophagy in a protein kinase AMP-activated catalytic subunit  $\alpha$ 2 (AMPK)/unc-51 like autophagy activating kinase 1-dependent and mTOR-independent manner (4). Furthermore, ginsenoside Rg2 increased autophagy in MCF-7 cells *in vitro* (5). Additionally, it was reported that ginsenoside Rg2 exhibited protective effects against hydrogen peroxide-induced injury and apoptosis in human cardiomyocytes (HCMs) (6).

Trastuzumab (TzM) is a humanized monoclonal antibody that targets the extracellular domain of human epidermal growth factor receptor 2 (HER2) and exerts significant therapeutic effects in early-stage HER2-positive breast cancer (7). TzM significantly improves the overall survival of the majority of patients with HER2-positive breast cancer (8). However, despite its beneficial effects, TzM is associated with several cardiac side effects, including congestive heart failure, hypertension, thromboembolic disease, ischemic heart disease, QT prolongation and bradycardia (9,10).

The present study aimed to investigate whether ginsenoside Rg2 could protect HCMs against TzM-induced toxicity *in vitro*. The results may improve the care of patients with breast cancer treated with TzM.

## Materials and methods

**Cell culture.** Human primary HCMs (Applied Biological Materials, Inc.) were cultured in DMEM (Sigma-Aldrich; Merck KGaA) containing 10% FBS (Thermo Fisher Scientific, Inc.) and 1% streptomycin-penicillin, and maintained at 37°C and 5% CO<sub>2</sub>. Upon reaching 80% confluency, HCMs were pretreated with 200  $\mu$ M ginsenoside Rg2 [purity >98% (by high-performance liquid chromatography analysis); MedChemExpress] for 12 h at 37°C, followed by exposure to 100  $\mu$ g/ml TzM (Roche Diagnostics) for 24 h at 37°C.

**Cell proliferation assay.** HCMs (5x10<sup>3</sup> cells/well) were seeded in a 96-well plate in triplicate. The cells were subsequently treated with TzM (0, 10, 50, 100 or 200  $\mu$ g/ml),

*Correspondence to:* Dr Xiaoyong Qi, Department of Cardiovascular Medicine, Hebei General Hospital, 348 West Heping Road, Shijiazhuang, Hebei 050000, P.R. China  
E-mail: xiaoyongqi28@126.com

**Key words:** trastuzumab, ginsenoside Rg2, apoptosis, autophagy

ginsenoside Rg2 (0, 50, 100, 200, or 300  $\mu$ M), a combination of 200  $\mu$ M ginsenoside Rg2 and 100  $\mu$ g/ml TZM or a combination of ginsenoside 200  $\mu$ M Rg2, 100  $\mu$ g/ml TZM and 5 mM 3-methyladenine (3-MA; Sigma-Aldrich; Merck KGaA) for 24 h at 37°C. Following treatment, the cells were further incubated with 10  $\mu$ l Cell Counting Kit-8 (CCK-8) solution (Dojindo Molecular Technologies, Inc.) at 37°C for 3 h and the absorbance was measured at a wavelength of 490 nm using a microplate reader. The cells in the control group were not given any treatment. IC<sub>50</sub> values were determined using GraphPad Prism software (version 7.0; GraphPad Software, Inc.).

**Apoptosis assay.** Cell apoptosis was detected using a propidium iodide (PI) and Annexin V staining kit (BD Biosciences) according to the manufacturer's protocol. Briefly, 2x10<sup>5</sup> HCMs were seeded in a 6-well plate and then treated with 50 or 100  $\mu$ g/ml TZM for 24 h and were subsequently harvested and washed twice with cold PBS. Subsequently, the cells were resuspended in binding buffer and stained with 2  $\mu$ l Annexin V and 2  $\mu$ l PI for 15 min at 25°C in the dark. The cell apoptosis rate was determined using a FACSCanto II flow cytometer (BD Biosciences) and BD CellQuest™ Pro software (version 5.1; BD Biosciences).

**Western blotting.** HCMs were rinsed and lysed using RIPA lysis buffer (EMD Millipore) containing a protease and phosphatase inhibitor. Subsequently, the cell lysates were vortexed on ice five times within 20 min and centrifuged for 10 min at 10,000 x g at 4°C. The protein concentration was determined using a bicinchoninic acid protein quantification kit (Promega Corporation). Protein aliquots (30  $\mu$ g) were subjected to SDS-PAGE on a 10% gel and subsequently transferred onto PVDF membranes (EMD Millipore). The membranes were blocked using 5% non-fat milk for 1 h at room temperature. The membranes were then incubated with the following primary antibodies: Anti-phosphorylated (p)-AKT (cat. no. ab38449), anti-p-mTOR (cat. no. ab84400), anti-autophagy protein 5 (ATG5, cat. no. ab109490), anti-beclin 1 (cat. no. ab210498), anti-microtubule associated protein 1 light chain 3 $\alpha$  (LC3, cat. no. ab62721) overnight at 4°C. All primary antibodies were used at a 1:200 dilution and were purchased from Abcam. Following washing with PBS, the membranes were incubated with horseradish peroxidase-conjugated secondary antibodies (Abcam) for 1 h at room temperature. An ECL reagent kit (Santa Cruz Biotechnology, Inc.) was used to visualize the immunoreactive bands according to the manufacturer's protocol. Protein band intensities were quantified using ImageJ software (v1.8.0.112; National Institutes of Health).  $\beta$ -actin (1:200 dilution; cat. no. ab8227; Abcam) acted as the internal control.

**Immunofluorescence staining.** Following exposure to the aforementioned treatments, HCMs were washed with PBS three times and fixed with 100% methanol for 10 min at room temperature. Next, cells were washed three times with PBS and permeabilized with 1% Triton X-100 (Sigma-Aldrich; Merck KGaA) for 10 min at room temperature. The cells were subsequently blocked with 4% BSA (Sigma-Aldrich; Merck KGaA) in PBS for 1 h at room temperature and incubated with primary antibodies against Ki67 (1  $\mu$ g/ml; cat. no. ab15580; Abcam) or LC3 (1  $\mu$ g/ml; cat. no. ab192890;

Abcam) for 2 h at 4°C. Following primary antibody incubation, cells were incubated with a FITC-conjugated anti-rabbit IgG secondary antibody (1:5,000; cat. no. 150077; Abcam) for 1 h at room temperature. Finally, the cells were washed three times with PBS and stained with DAPI (Vector Laboratories, Inc.) for 5 min at room temperature. The cells were imaged using a fluorescence microscope (magnification, x200) and the number of nuclei and Ki67-positive cells were counted in three randomly-selected fields.

**Monodansylcadaverine (MDC) staining.** A total of 2x10<sup>5</sup> HCMs were seeded in a 6-well plate and then treated with different concentrations of TZM or a combination of TZM and ginsenoside Rg2. Cells were then labeled with MDC (50  $\mu$ M) in PBS for 10 min at 37°C in the dark. After washing with PBS three times, cells were fixed in 4% PFA for 30 min at room temperature. Subsequently, the cells were visualized under a fluorescence microscope (magnification, x200).

**Statistical analysis.** Statistical analyses were performed using SPSS software (version 17.0; SPSS, Inc.). Data are expressed as the mean  $\pm$  SD of three replicates. Comparisons among multiple groups were made with the one-way ANOVA followed by Tukey's post hoc test. P<0.05 was considered to indicate a statistically significant difference.

## Results

**TZM inhibits the proliferation of HCMs by inhibiting the Akt/mTOR signaling pathway.** HCMs were treated with increasing concentrations of TZM (0, 10, 50, 100 or 200  $\mu$ g/ml) for 24 h, and the effects of TZM on cell proliferation were measured using a CCK-8 assay. The results revealed that 50, 100 or 200  $\mu$ g/ml TZM significantly decreased cell proliferation compared with the control group (Fig. 1A). These data suggested that TZM inhibited the proliferation of HCMs in a dose-dependent manner, with an IC<sub>50</sub> value of 88  $\mu$ g/ml. Annexin V/PI staining was subsequently performed to determine the percentage of apoptotic cells following treatment with 50 or 100  $\mu$ g/ml TZM. As indicated in Fig. 1B and C, a significant increase in apoptotic cells was observed in TZM-treated cells compared with the controls. Furthermore, western blotting revealed that the levels of p-Akt and p-mTOR in cells were significantly decreased following treatment with TZM compared with controls (Fig. 1D-F). Therefore, 100  $\mu$ g/ml TZM was used for subsequent experiments. These results suggested that TZM could induce apoptosis of HCMs by inhibiting the Akt/mTOR signaling pathway.

**TZM-induced cytotoxicity in HCMs is reversed by ginsenoside Rg2.** The chemical structure of ginsenoside Rg2 is presented in Fig. 2A. A CCK-8 assay was performed to evaluate the effects of ginsenoside Rg2 or the combination of ginsenoside Rg2 and TZM on HCM proliferation. The results indicated that ginsenoside Rg2 (at concentrations between 0-200  $\mu$ M) exhibited no cytotoxicity (Fig. 2B). Therefore, 200  $\mu$ M ginsenoside Rg2 was used for subsequent experiments. Pretreatment with ginsenoside Rg2 significantly reversed TZM-induced cytotoxicity compared with TZM alone (Fig. 2C).

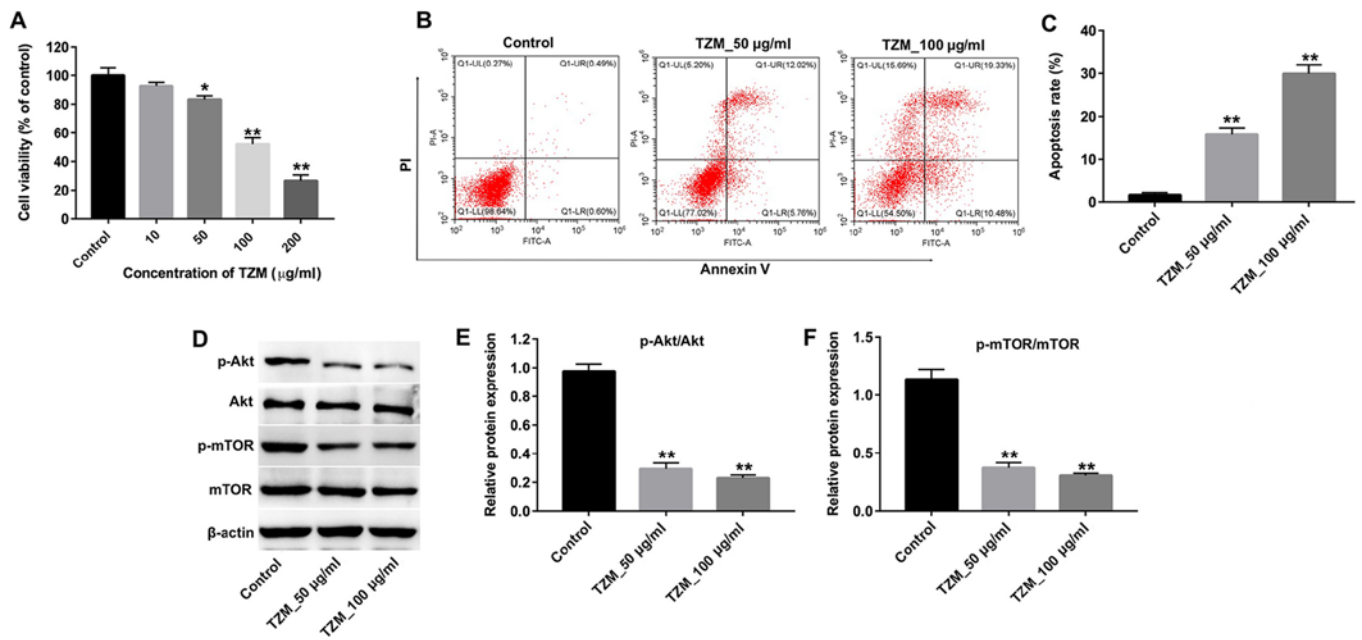


Figure 1. TZM inhibits the proliferation of HCMs by inhibiting the Akt/mTOR signaling pathway. (A) HCMs were treated with different concentrations of TZM (0, 10, 50, 100 or 200  $\mu\text{g/ml}$ ) for 24 h, and cell proliferation was examined using a Cell Counting Kit-8 assay. (B) HCMs were incubated with 0, 50 or 100  $\mu\text{g/ml}$  TZM for 24 h, and apoptotic cells were detected with Annexin V/PI staining and flow cytometry. (C) Quantification of Annexin V-positive cells. (D) Cells were treated with 0, 50 or 100  $\mu\text{g/ml}$  TZM for 24 h, and the expression of p-Akt and p-mTOR protein was measured by western blotting. The relative levels of (E) p-Akt and (F) p-mTOR were normalized to Akt and mTOR, respectively and quantified using ImageJ software. Data were representative of three separate experiments. \* $P < 0.05$  and \*\* $P < 0.01$  vs. the control group. TZM, trastuzumab; HCM, human cardiomyocyte; PI, propidium iodide; p, phosphorylated.

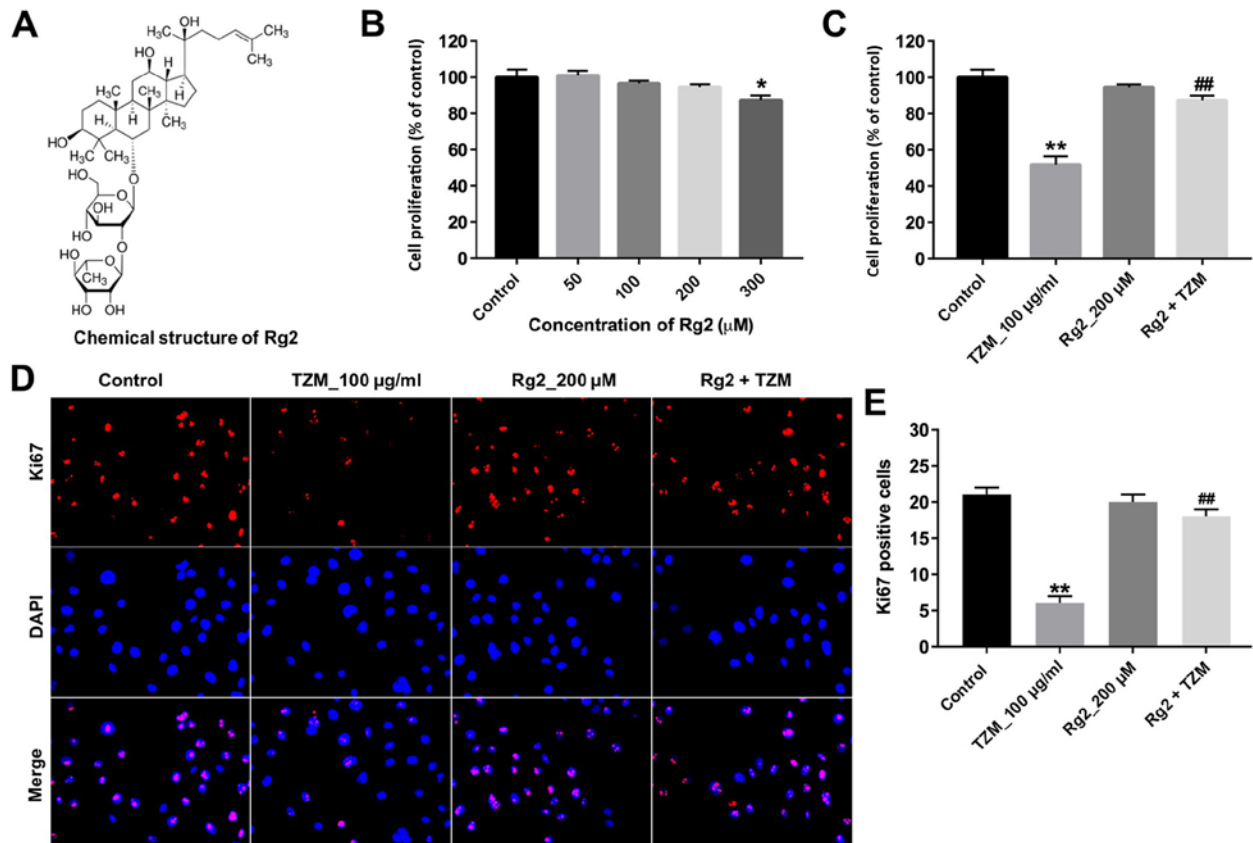


Figure 2. TZM-induced cytotoxicity is reversed by ginsenoside Rg2. (A) Chemical structure of ginsenoside Rg2. (B) HCMs were incubated with 0, 50, 100, 200 or 300  $\mu\text{M}$  ginsenoside Rg2 for 12 h, and cell proliferation was examined with a CCK-8 assay. (C) HCMs were incubated with ginsenoside Rg2 and/or TZM at the indicated time points and cell proliferation was assessed using a CCK-8 assay. (D) Cell proliferation was detected by immunofluorescence staining with DAPI and Ki67. Representative micrographs of Ki67-positive HCMs (red) and DAPI staining (blue) of the nuclei. magnification,  $\times 200$  (E) The percentage of Ki67-positive HCMs was calculated from three randomly-captured images for each group after treatment. \* $P < 0.05$  and \*\* $P < 0.01$  vs. the control group; ## $P < 0.01$  vs. the TZM group. TZM, trastuzumab; HCM, human cardiomyocyte; CCK-8, Cell Counting Kit-8; Rg2, ginsenoside Rg2.

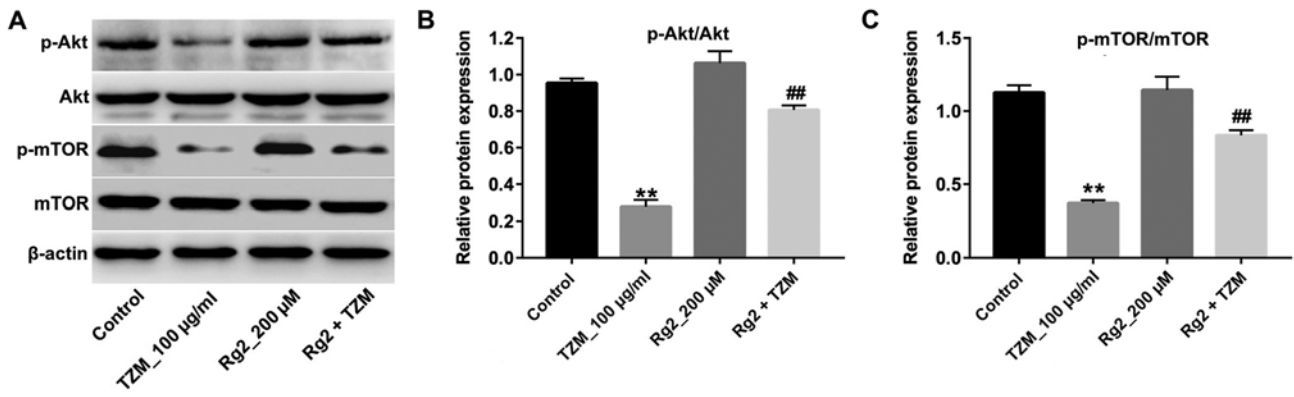


Figure 3. Akt/mTOR pathway inhibition effect of TZM is reversed by ginsenoside Rg2. (A) HCMs were incubated with 200  $\mu$ M ginsenoside Rg2 for 12 h and exposed to 100  $\mu$ g/ml TZM for another 24 h. The expression of p-Akt and p-mTOR in cells was measured by western blotting. The relative levels of (B) p-Akt and (C) p-mTOR were normalized to Akt and mTOR, respectively and quantified using ImageJ software. Data are representative of three independent experiments. \*\* $P < 0.01$  vs. the control group; ## $P < 0.01$  vs. the TZM group. TZM, trastuzumab; HCM, human cardiomyocyte; p, phosphorylated; Rg2, ginsenoside Rg2.

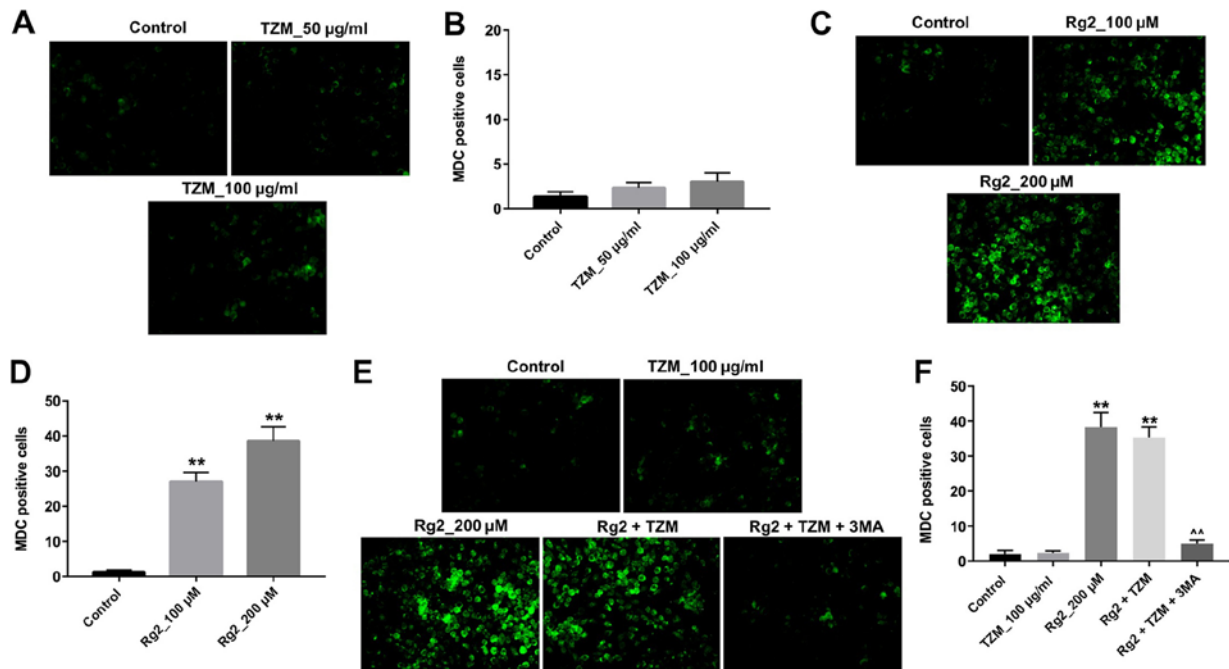


Figure 4. Ginsenoside Rg2 induces autophagy of HCMs. (A) HCMs were labeled with MDC after incubation with 0, 50 or 100  $\mu$ g/ml TZM for 24 h. Magnification, x200. (B) Quantitative analysis of MDC-positive cells in (A). (C) HCMs were labeled with MDC after incubation with 0, 100 or 200  $\mu$ M ginsenoside Rg2 for 12 h. Magnification, x200. (D) Quantitative analysis of MDC-positive cells in (C). (E) HCMs were exposed to 200  $\mu$ M ginsenoside Rg2 with or without 5 mM 3-MA for 12 h and exposed to 100  $\mu$ g/ml TZM for another 24 h. Cell autophagy was then detected with MDC staining. Magnification, x200. (F) Quantitative analysis of MDC-positive cells from (E). Data are representative of three independent experiments. \*\* $P < 0.01$  vs. the control group. ^^ $P < 0.01$  vs. the Rg2 + TZM group. TZM, trastuzumab; HCM, human cardiomyocyte; MDC, monodansylcadaverine; 3-MA, 3-methyladenine; Rg2, ginsenoside Rg2.

HCMs were subsequently subjected to immunofluorescence staining. Ki67 expression was significantly increased in the ginsenoside Rg2-pretreated group compared with the TZM group (Fig. 2D and E). Furthermore, TZM-induced p-Akt and p-mTOR downregulation was significantly reversed by ginsenoside Rg2 compared with the TZM group (Fig. 3A-C). Collectively, these results suggested that ginsenoside Rg2 may significantly alleviate TZM-induced cardiotoxicity by upregulating the Akt/mTOR signaling pathway.

*Ginsenoside Rg2 induces autophagy of HCMs.* MDC is a selective fluorescent marker that labels autophagic vacuoles (11).

To further explore the mechanisms underlying the protective effect of ginsenoside Rg2 against TZM cytotoxicity, MDC fluorescence staining was performed. The results revealed that MDC fluorescence was barely detected in HCMs incubated with TZM (Fig. 4A and B), whereas strong MDC fluorescence was observed in ginsenoside Rg2-treated cells (Fig. 4C and D). Furthermore, the combination of ginsenoside Rg2 and TZM significantly increased the levels of MDC fluorescence compared with the control group, which were subsequently significantly decreased in the presence of the autophagy inhibitor 3-MA (Fig. 4E and F). Therefore, the results suggested that ginsenoside Rg2 may significantly induce autophagy in HCMs.



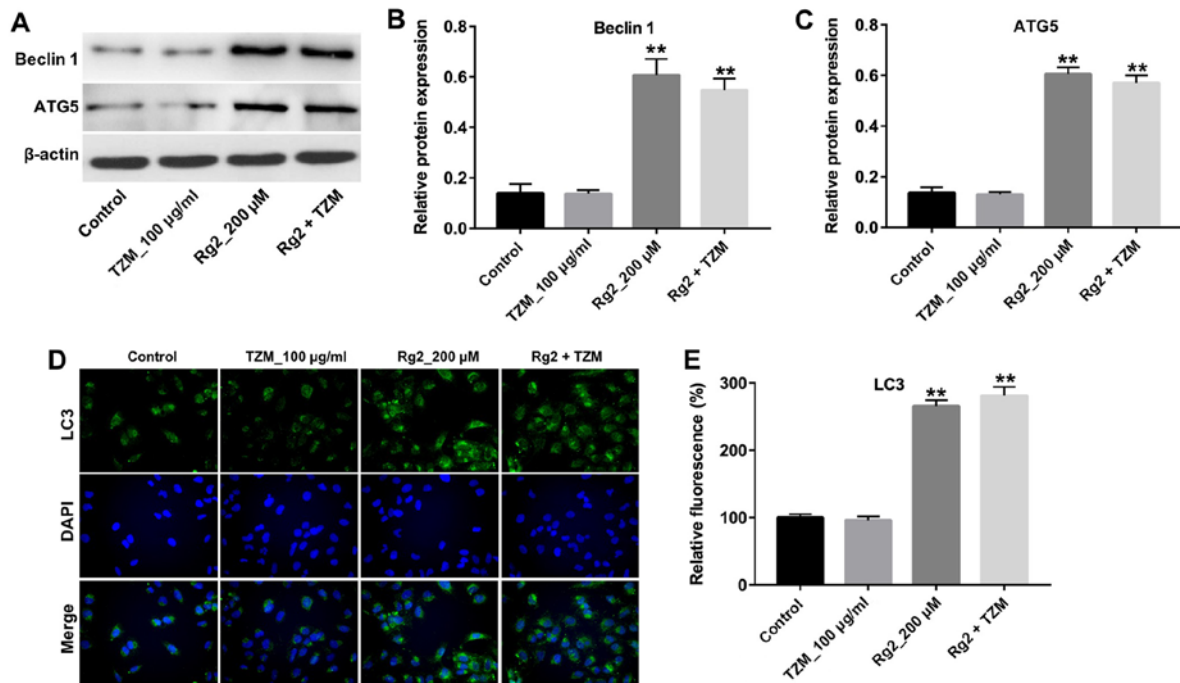


Figure 5. Ginsenoside Rg2 increases the expression of autophagy-related proteins beclin 1, LC3 and ATG5. (A) HCM cells were incubated with 200  $\mu$ M ginsenoside Rg2 for 12 h and exposed to 100  $\mu$ g/ml TZM for another 24 h. The expression levels of beclin 1, LC3 and ATG5 were measured by western blotting. The relative levels of (B) beclin 1 and (C) ATG5 were normalized to  $\beta$ -actin and quantified using ImageJ software. (D) The expression of LC3 in cells was detected with immunofluorescence staining. Magnification,  $\times 200$ . (E) Quantification of LC3-positive cells. Data were representative of three separate experiments. \*\* $P < 0.01$  vs. the control group. TZM, trastuzumab; HCM, human cardiomyocyte; LC3, microtubule associated protein 1 light chain 3  $\alpha$ ; ATG5, autophagy protein 5; Rg2, ginsenoside Rg2.

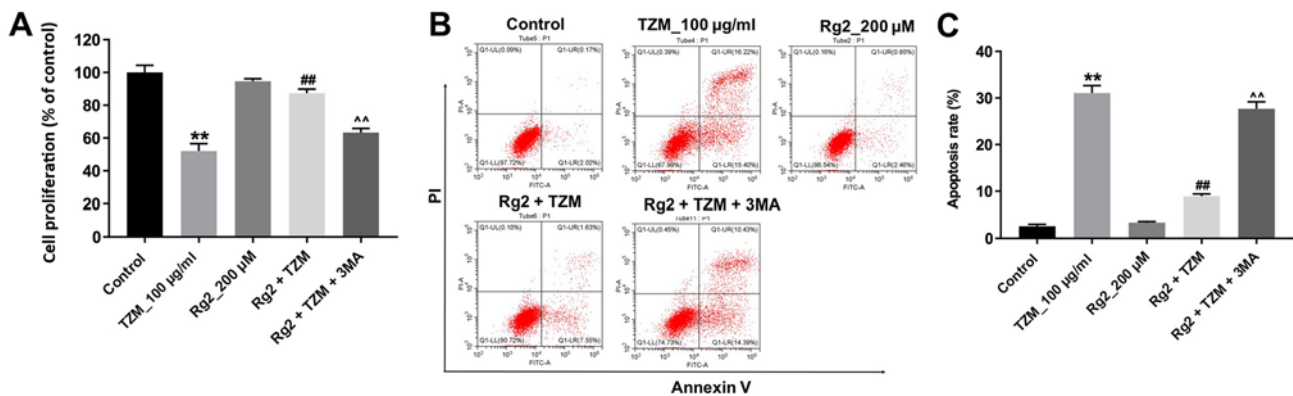


Figure 6. Inhibition of autophagy abolishes the protective effect of ginsenoside Rg2 against TZM in HCMs. (A) HCMs were exposed to 200  $\mu$ M ginsenoside Rg2 with or without 5 mM 3-MA for 12 h and exposed to 100  $\mu$ g/ml TZM for another 24 h. Cell proliferation was examined with a Cell Counting Kit-8 assay. (B) Apoptotic cells were detected using Annexin V/PI staining. (C) Quantification of apoptotic cells. \*\* $P < 0.01$  vs. the control group; ## $P < 0.01$  vs. the TZM group; ^^ $P < 0.01$  vs. the Rg2 + TZM group. TZM, trastuzumab; HCM, human cardiomyocyte; 3-MA, 3-methyladenine; PI, propidium iodide; Rg2, ginsenoside Rg2.

*Ginsenoside Rg2 increases the expression of the autophagy-related proteins beclin 1, LC3 and ATG5 in HCMs.* To further explore the mechanisms underlying ginsenoside Rg2-induced autophagy, the expression of the key autophagy markers beclin 1, LC3 and ATG5 was detected by western blotting. As indicated in Fig. 5A-C, treatment with TZM did not significantly affect the expression of beclin 1 and ATG5 in cells compared with controls; however, the levels of beclin1 and ATG5 were significantly increased in ginsenoside Rg2-treated cells compared with controls. In addition, the results of immunofluorescence staining indicated

the nuclear expression of LC3 was significantly increased following Rg2 treatment (Fig. 5D and E). These data further demonstrated that ginsenoside Rg2 increased autophagy in HCMs by increasing the expression of the autophagy-related proteins beclin 1, LC3 and ATG5.

*Inhibition of autophagy in HCMs abolished the protective effect of ginsenoside Rg2 against TZM.* To verify whether ginsenoside Rg2 exerted a protective effect against TZM in HCMs by inducing autophagy, the effects of the autophagy inhibitor 3-MA were investigated. As indicated in Fig. 6A, the

protective effects of ginsenoside Rg2 against TZM-induced cytotoxicity in HCMs were reversed by 3-MA. Meanwhile, the antiapoptotic effects of ginsenoside Rg2 in TZM-stimulated HCMs were also alleviated by 3-MA (Fig. 6B and C). These data indicated that ginsenoside Rg2 could attenuate TZM-induced cytotoxicity in HCMs by inducing autophagy.

## Discussion

The present study established an *in vitro* model of TZM-induced toxicity in HCMs. TZM decreased cell proliferation, increased apoptosis and decreased the expression of p-Akt and p-mTOR. However, TZM-induced cytotoxicity and p-Akt and p-mTOR downregulation were reversed by ginsenoside Rg2. In addition, ginsenoside Rg2 significantly induced autophagy in HCMs by increasing the levels of beclin 1, LC3 and ATG5. The present study revealed that ginsenoside Rg2 may protect HCMs from TZM-induced toxicity by activating autophagy.

It was hypothesized that ginsenoside Rg2 has anti-oxidant, antidiabetic, antiapoptotic and neuroprotective activities (3,12,13). A previous study reported that ginsenoside Rg2 exerted protective effects against hydrogen peroxide-induced injury and apoptosis in HCMs (6). Furthermore, ginsenoside Rg2 increased autophagy and activated the p53/AMPK signaling pathway in MCF-7 breast cancer cells (5). Moreover, ginsenoside Rg2 decreased lipopolysaccharide-induced Bax and caspase-3 and -9 expression, and exerted an antiapoptotic effect in neurons (14). Kang *et al* (15) found that ginsenoside Rg2 could protect HaCaT cells from UV-B-induced cell damage. Meanwhile, Wang *et al* (16) indicated that ginsenoside Rg2 could inhibit the proliferation of breast cancer cells *in vitro*. The aforementioned studies indicated that ginsenoside Rg2 exhibited dual functions in protecting cells from DNA damage and inducing apoptosis in cancer cells. The present study investigated whether pretreatment with ginsenoside Rg2 could reverse TZM-induced toxicity in HCMs. The results revealed that ginsenoside Rg2 exhibited protective effects against TZM-induced toxicity by inducing autophagy in HCMs. Moreover, to the best of our knowledge, the present study was the first to demonstrate that ginsenoside Rg2 exhibited protective effects against TZM-induced toxicity in HCMs.

Beclin 1, LC3 and ATG5 are autophagy-related proteins required for autophagosome elongation (17). In the present study, pretreatment with ginsenoside Rg2 increased the levels of beclin 1, LC3 and ATG5, which indicated that TZM-induced toxicity was reversed by ginsenoside Rg2 by increasing autophagy. A previous study revealed that p-53 and p-AMPK were involved in ginsenoside Rg2-induced autophagy in MCF-7 cells (5). However, in the present study, pretreatment with ginsenoside Rg2 reversed TZM-induced downregulation of p-Akt and p-mTOR in HCMs. It was reported that canonical autophagy requires mTOR inhibition (18). Moreover, the Akt/mTOR signaling pathway is one of the main downstream effectors of HER2 (19). Previous studies demonstrated that TZM exerted antitumor activities by inhibiting the Akt/mTOR signaling pathway in HER2-overexpressing breast cancer cells (20,21). In the present study, treatment with ginsenoside Rg2 alone had no effect on the Akt/mTOR signaling pathway in HCMs. The

inhibition of the Akt/mTOR signaling pathway induced by TZM was reversed by ginsenoside Rg2. Evidence has shown that the AKT/mTOR pathway plays an important role in several cellular processes, including proliferation, survival and autophagy (22). Hu *et al* (23) found that inhibition of autophagy promoted advanced glycation end product-induced apoptosis in cardiomyocytes by inhibiting the AKT/mTOR signaling. In the present study, TZM-induced p-Akt and p-mTOR protein decreases were significantly reversed by ginsenoside Rg2 treatment, indicating that ginsenoside Rg2 could induce autophagy of HCM cells by activating the AKT/mTOR pathway. Meanwhile, the anti-apoptotic effects of ginsenoside Rg2 in TZM-stimulated HCMs cells were reversed by 3-MA treatment, indicating that inhibition of autophagy abolished the protective effect of ginsenoside Rg2 against TZM in HCMs. The results suggested that the mechanism by which ginsenoside Rg2 protected against TZM-induced cardiotoxicity was reversed by inhibition of the Akt/mTOR signaling pathway.

Collectively, the results obtained in the present study revealed that ginsenoside Rg2 exhibited protective effects against TZM-induced toxicity in HCMs by activating autophagy and increasing the expression of Akt and mTOR. Ginsenoside Rg2 may serve as a potential clinical agent to prevent TZM-related cardiotoxicity and may provide significant beneficial effects for patients with breast cancer. However, the data presented in this study requires further *in vivo* validation prior to the clinical application of ginsenoside Rg2.

## Acknowledgements

Not applicable.

## Funding

No funding was received.

## Availability of data and materials

The datasets used and/or analyzed during the current study are available from the corresponding author on reasonable request.

## Authors' contributions

GL made major contributions to the conception, design and manuscript drafting of this study. GL, XL and FS were responsible for data acquisition, data analysis, data interpretation and manuscript revision. XQ made substantial contributions to conception and design of the study and revised the manuscript. All authors agreed to be accountable for all aspects of the work. All authors read and approved the final manuscript.

## Ethics approval and consent to participate

Not applicable.

## Patient consent for publication

Not applicable.

## Competing interests

The authors declare that they have no competing interests.

## References

- Xu QM, Jia D, Gao HW, Zhang MM, He WJ, Pan S, Liu YL, Li XR, Cui JH and Yang SL: In vitro and in vivo protective effects of ginsenosides on acute renal injury induced by cantharidin. *J Functional Foods* 5: 2012-2018, 2013.
- Chen XJ, Zhang XJ, Shui YM, Wan JB and Gao JL: Anticancer activities of protopanaxadiol- and protopanaxatriol-type ginsenosides and their metabolites. *Evid Based Complement Alternat Med* 2016: 5738694, 2016.
- Zhang G, Liu A, Zhou Y, San X, Jin T and Jin Y: *Panax ginseng* ginsenoside-Rg2 protects memory impairment via anti-apoptosis in a rat model with vascular dementia. *J Ethnopharmacol* 115: 441-448, 2008.
- Fan Y, Wang N, Rocchi A, Zhang W, Vassar R, Zhou Y and He C: Identification of natural products with neuronal and metabolic benefits through autophagy induction. *Autophagy* 13: 41-56, 2017.
- Chung Y, Jeong S, Choi HS, Ro S, Lee JS and Park JK: Upregulation of autophagy by Ginsenoside Rg2 in MCF-7 cells. *Anim Cells Syst (Seoul)* 22: 382-389, 2018.
- Fu W, Sui D, Yu X, Gou D, Zhou Y and Xu H: Protective effects of ginsenoside Rg2 against H<sub>2</sub>O<sub>2</sub>-induced injury and apoptosis in H9c2 cells. *Int J Clin Exp Med* 8: 19938-19947, 2015.
- Gershon N, Berchenko Y, Hall PS and Goldstein DA: Cost effectiveness and affordability of trastuzumab in sub-Saharan Africa for early stage. *Cost Eff Resour Alloc* 17: 5, 2019.
- Slamon D, Eiermann W, Robert N, Pienkowski T, Martin M, Press M, Mackey J, Glaspy J, Chan A, Pawlicki M, *et al*: Adjuvant trastuzumab in HER2-positive breast cancer. *N Engl J Med* 365: 1273-1283, 2011.
- Mazzotta M, Krasniqi E, Barchiesi G, Pizzuti L, Tomao F, Barba M and Vici P: Long-term safety and real-world effectiveness of trastuzumab in breast cancer. *J Clin Med* 8: 254, 2019.
- Sato A, Yoshihisa A, Miyata-Tatsumi M, Oikawa M, Kobayashi A, Ishida T, Ohtake T and Takeishi Y: Valvular heart disease as a possible predictor of trastuzumab-induced cardiotoxicity in patients with breast cancer. *Mol Clin Oncol* 10: 37-42, 2019.
- Biederbick A, Kern HF and Elsässer HP: Monodansylcadaverine (MDC) is a specific in vivo marker for autophagic vacuoles. *Eur J Cell Biol* 66: 3-14, 1995.
- Jeong SJ, Han SH, Kim DY, Lee JC, Kim HS, Kim BH, Lee JS, Hwang EH and Park JK: Effects of mRg2, a mixture of ginsenosides containing 60% Rg2, on the ultraviolet B-induced DNA repair synthesis and apoptosis in NIH3T3 cells. *Int J Toxicol* 26: 151-158, 2007.
- Ye J, Yao JP, Wang X, Zheng M, Li P, He C, Wan JB, Yao X and Su H: Neuroprotective effects of ginsenosides on neural progenitor cells against oxidative injury. *Mol Med Rep* 13: 3083-3091, 2016.
- Chung YH, Jeong SA, Choi HS, Ro S, Lee JS and Park JK: Protective effects of ginsenoside Rg2 and astaxanthin mixture against UVB-induced DNA damage. *Anim Cells Syst (Seoul)* 22: 400-406, 2018.
- Kang HJ, Huang YH, Lim HW, Shin D, Jang K, Lee Y, Kim K and Lim CJ: Stereospecificity of ginsenoside Rg2 epimers in the protective response against UV-B radiation-induced oxidative stress in human epidermal keratinocytes. *J Photochem Photobiol B* 165: 232-239, 2016.
- Wang CZ, Aung HH, Zhang B, Sun S, Li XL, He H, Xie JT, He TC, Du W and Yuan CS: Chemopreventive effects of heat-processed *Panax quinquefolius* root on human breast cancer cells. *Anticancer Res* 28: 2545-2551, 2008.
- Mondaca-Ruff D, Riquelme JA, Quiroga C, Norambuena-Soto I, Sanhueza-Olivares F, Villar-Fincheira P, Hernández-Díaz T, Cancino-Arenas N, San Martín A, García L, *et al*: Angiotensin II-regulated autophagy is required for vascular smooth muscle cell hypertrophy. *Front Pharmacol* 9: 1553, 2019.
- Gatica D, Chiong M, Lavandero S and Klionsky DJ: Molecular mechanisms of autophagy in the cardiovascular system. *Circ Res* 116: 456-467, 2015.
- Sukawa Y, Yamamoto H, Noshio K, Ito M, Igarashi H, Naito T, Mitsuhashi K, Matsunaga Y, Takahashi T, Mikami M, *et al*: HER2 expression and PI3K-Akt pathway alterations in gastric cancer. *Digestion* 89: 12-17, 2014.
- Yang Y, Ren F, Tian Z, Song W, Cheng B and Feng Z: Osthole synergizes with HER2 inhibitor, trastuzumab in HER2-overexpressed N87 Gastric cancer by inducing apoptosis and inhibition of AKT-MAPK pathway. *Front Pharmacol* 9: 1392, 2018.
- Han S, Meng Y, Tong Q, Li G, Zhang X, Chen Y, Hu S, Zheng L, Tan W, Li H, *et al*: The ErbB2-targeting antibody trastuzumab and the small-molecule SRC inhibitor saracatinib synergistically inhibit ErbB2-overexpressing gastric cancer. *MABs* 6: 403-408, 2014.
- Yu JS and Cui W: Proliferation, survival and metabolism: The role of PI3K/AKT/mTOR signalling in pluripotency and cell fate determination. *Development* 143: 3050-3060, 2016.
- Hu P, Zhou H, Lu M, Dou L, Bo G, Wu J and Huang S: Autophagy plays a protective role in advanced glycation end product-induced apoptosis in cardiomyocytes. *Cell Physiol Biochem* 37: 697-706, 2015.



This work is licensed under a Creative Commons Attribution-NonCommercial-NoDerivatives 4.0 International (CC BY-NC-ND 4.0) License.